

# The radio expansion and brightening of the very young supernova remnant G1.9 + 0.3

D. A. Green,<sup>1\*</sup> S. P. Reynolds,<sup>2</sup> K. J. Borkowski,<sup>2</sup> U. Hwang,<sup>3</sup> I. Harrus<sup>3</sup>  
and R. Petre<sup>3</sup>

<sup>1</sup>*Astrophysics Group, Cavendish Laboratory, 19 J. J. Thomson Avenue, Cambridge CB3 0HE*

<sup>2</sup>*Department of Physics, North Carolina State University, Raleigh NC 27695-8202, USA*

<sup>3</sup>*NASA/GSFC, Code 660, Greenbelt, MD 2077, USA*

Accepted 2008 April 14. Received 2008 April 10

## ABSTRACT

Recent radio observations of the small Galactic supernova remnant G1.9 + 0.3 made at 4.86 GHz with the Very Large Array are presented, and compared with earlier observations at 1.49 GHz which have a comparable resolution ( $10 \times 4$  arcsec<sup>2</sup>). These show that the radio emission from this remnant has expanded significantly, by about 15 per cent over 23 yr, with a current outer diameter of  $\approx 92$  arcsec. This expansion confirms that G1.9 + 0.3 is the youngest Galactic remnant yet identified, only about 150 yr old at most. Recent, lower resolution, 1.43-GHz observations are also discussed, and the integrated flux densities from these and the 4.86-GHz observations are compared with earlier results. This shows that the integrated flux density of G1.9 + 0.3 has been increasing recently.

**Key words:** ISM: individual: G1.9 + 0.3 – supernova remnants – radio continuum: ISM.

## 1 INTRODUCTION

The small Galactic ‘shell’ type supernova remnant (SNR) G1.9 + 0.3 was identified by Green & Gull (1984), from Very Large Array (VLA) observations of a sample of Galactic radio sources. It was revealed as a small limb-brightened shell, brighter in the north, only just over 1 arcmin in diameter, and is the smallest catalogued Galactic SNR (Green 2004<sup>1</sup>). Although its distance was not known at the time of its identification, it was clear that it must be a young SNR, due to its small physical size (e.g. even at distance as large as 17 kpc – that is, twice the distance to the Galactic Centre – its physical diameter would be  $\approx 6$  pc, which is comparable to that of the remnant of Tycho’s SN of AD 1572). As such G1.9 + 0.3 is one of few ‘young but distant’ SNRs, which are missing from current catalogues, due to selection effects (e.g. Green 2005), but perhaps also indicating a true deficit (The et al. 2006). Searches for these missing young remnants have had limited success (see Green & Gull 1984; Helfand et al. 1984; Green 1985, 1989; Sramek et al. 1992; Misanovic, Cram & Green 2002, see also Saikia et al. 2004).

There are few published observations of G1.9 + 0.3 in the literature. VLA images at 4.9 and 1.5 GHz (from observations made in 1985) are presented in Green & Gull (1984) and Green (2004), respectively. Gray (1994a) presents MOST observations at 843 MHz, but these barely resolve the remnant. Nord et al. (2004) and Yusef-Zadeh, Hewitt & Cotton (2004) present VLA observations, at

330 MHz and 1.5 GHz, respectively, but of limited quality or resolution. G1.9 + 0.3 has also been detected in X-rays, with *ASCA* as AX J1748.7–2709 (Sakano et al. 2002).

Recently, *Chandra* observations (Reynolds et al. 2008, hereafter Paper I) have revealed that G1.9 + 0.3 is one of the few shell SNRs that have line-free X-ray emission, dominated by synchrotron rather than thermal emission. The size of the X-ray emission observed by *Chandra* was, unusually, significantly larger than the then published radio observations, which were interpreted in Paper I as requiring a large expansion rate –  $\approx 16$  per cent over 23 yr – which implies that G1.9 + 0.3 is a very young SNR. Here we present recent new radio observations made with the VLA, which in comparison with previous observations at a similar resolution, but a different frequency, confirm the large expansion rate, and hence youth of this remnant. We also discuss the temporal evolution of the flux density of G1.9 + 0.3, and conclude that it has been brightening over recent decades.

## 2 OBSERVATIONS

G1.9 + 0.3 was recently observed with the VLA at 4.86 GHz in the C-array configuration. The resolutions of these observations closely match those of VLA observations made in 1985 at 1.49 GHz in the B-array configuration (results from which are shown in Green 2004). Details of these observations are given in Table 1. The new observations were processed using standard techniques in (classic) AIPS (see Bridle & Greisen 1994). Obviously corrupted data were flagged, the flux scale calibration was based on observations of 3C286, and antenna-based amplitude and phase calibrations from observations

\*E-mail: dag@mrao.cam.ac.uk

<sup>1</sup> See also <http://www.mrao.cam.ac.uk/surveys/snrs/> for an updated version (from 2006 April).

**Table 1.** VLA observations of G1.9 + 0.3.

	1985 observations	2008 observations
Date	1985 April 16	2008 March 12
VLA array	B	C
Frequency	1.49 GHz	4.86 GHz
Time on source	25 min	29 min
Primary calibrator	3C286	3C286
Assumed flux density	14.70 Jy	7.49 Jy
Secondary calibrator	B1829–106	J1751–251
Derived flux density	0.927 Jy	0.569 Jy

of calibrator source(s) made nearby in time were applied. The earlier 1.49-GHz observations were also reprocessed. Although the time spent observing G1.9 + 0.3 was similar in each observation, the details of the  $uv$ -coverage for the two observations are different, due to differences in LST coverage, missing antennas, and flagging of bad data. Consequently, the synthesized beams are slightly different. For expansion studies, comparison images were made at a matched resolution, see Fig. 1. These images show large expansion of the radio emission from G1.9 + 0.3, which is discussed further in Section 3.1. The positional alignment of these images was checked from the apparent position of a compact source that is about 1.4 arcmin north of the centre of the remnant. The positions of this source were found to be in agreement to better than 0.4 arcsec, which is small compared with the large changes seen between the 1985 and 2008 images of G1.9 + 0.3. It should be noted, however, the earlier 1.49-GHz observations probably do not have sufficient short baselines to be able to fully image the largest scale emission from G1.9 + 0.3. The VLA ‘Observational Status Summary’<sup>2</sup> lists the largest angular scale that ‘can be imaged reasonably well’ in a full synthesis as 2 arcmin for 1.49-GHz observations in the B-array, and notes that this value should be halved for single snapshot observations. Thus, given the angular size of G1.9 + 0.3 is over 1 arcmin, the largest scale structure may not be fully imaged in the 1.49-GHz observations. For the 4.86-GHz C-array observations, the largest angular scale well imaged with a full synthesis is 5 arcmin – since the C-array is not an exactly scaled version of B-array, but has better small baseline coverage – so even halving this for snapshot observations, the full emission from G1.9 + 0.3 should be well imaged. Indeed, from Fig. 1, the 1.49-GHz image shows extended negative artefacts, which are features of the limited small baseline coverage. The 4.86-GHz image is also better than the 1.49-GHz image, in terms of its sensitivity: the nominal noise on these images, from the rms away from bright emission, is about 0.038 and 0.012 mJy beam<sup>-1</sup> at 1.49 and 4.86 GHz, respectively.

Given the problem with missing large-scale emission in the 1.49-GHz observations, we also made some short 1.43-GHz observations of G1.9 + 0.3 in the same observation run as the 4.86-GHz observations, in order to investigate temporal variations in the flux density of G1.9 + 0.3. These consisted of two short ( $\approx 4$  min) scans of G1.9 + 0.3, together with adjacent calibration observations of 3C286 to set the overall flux density scale (with an assumed flux density of 14.7 Jy), and of the nearby secondary calibrator J1751–253 (for which a flux density of 1.18 Jy was derived). The results from these observations are discussed below in Section 3.2.

<sup>2</sup> Available via <http://www.vla.nrao.edu/>

### 3 DISCUSSION

#### 3.1 Expansion and structure

From Fig. 1, it is clear that there is a large expansion of the radio emission seen from G1.9 + 0.3 between 1985 and 2008. To quantify this, radial profiles of the emission from each image were constructed – see Fig. 2 – averaging over all angles, from a central position which was adjusted to maximize the peak of the radial profile from the 2008 image. (This position is  $17^{\text{h}}48^{\text{m}}45^{\text{s}}.4$ ,  $-27^{\circ}10'06''$ , J2000.0, which is close to the geometrical centre of the remnant.) A simple re-scaling of the 1985 radial profile indicates an average expansion of 15 per cent between 1985 and 2008, that is, 0.65 per cent yr<sup>-1</sup>, is required to match the positions of the peaks of the radial profiles (Fig. 2). This expansion rate is biased towards that appropriate to the brighter north and north-east portions of the remnant, since the radial profiles are weighted by intensity.

This result confirms that a significant expansion is needed to match the extent of the X-ray emission from the recent *Chandra* observations to older radio observations, as found in Paper I. Assuming free expansion, this implies an age of 150 yr for G1.9 + 0.3, which makes this the youngest known Galactic SNR (but also see Morris et al. 2006 and Renaud et al. 2006 for other possible very young SNRs which have been reported). As the remnant will have undergone some deceleration, this age is an upper limit. Very high X-ray absorption (Paper I) suggests that G1.9 + 0.3 is not much closer than the Galactic Centre, while the very high expansion would indicate a very large velocity if it were much farther away. Following Paper I, we adopt a nominal distance of 8.5 kpc, which for an age of  $\lesssim 150$  yr and a outer radio diameter of 92 arcsec corresponds to a mean expansion speed of  $\gtrsim 12\,000$  km s<sup>-1</sup>.

The interpretation of the radial profiles in simple terms of just a radial scaling is, however, complicated by a variety of effects. First, recall that the  $uv$ -coverage of these observations differ, particularly – as noted above – that the 1.49-GHz observations may not well image the large-scale emission from G1.9 + 0.3. Secondly, the images are at different frequencies, so that any change in spectral index across the remnant would appear as a relative change in emission between the epochs (e.g. a spectral index change of 0.05 would correspond to a relative intensity change of 6 per cent between 1.49 and 4.86 GHz). Thirdly, there are real changes in the emission over the 23 yr between the observations, so the changes seen are not just simple, self-similar expansion. In the case of G1.9 + 0.3, we are not observing the expansion of distinct features, such as the radio knots in Cas A (see Anderson & Rudnick 1995), or the well-defined outer shock of Tycho’s SNR (e.g. Tan & Gull 1985; Reynoso et al. 1997). From Fig. 1, there is evidence for changes in the shape and brightness of the radio emission between 1985 and 2008. This is particularly notable in the north-west, where there is a clear extension outside the brighter rim of emission from the remnant in the 2008 image (labelled ‘NW’ in Fig. 1). There is some indication of extension in the 1985 image, but at a much lower level than in the 2008 image. The azimuth range of this outer extension corresponds closely to where the X-ray emission shows a bright ‘ear’ in this region (Paper I; see Fig. 3 above). In the east, there is also a faint extension outside the main emission particularly in the 2008 image (labelled ‘E’), but over a much smaller azimuth range than the outer extension in the north-west. Also, the ridge line of the emission in the north-east clearly differs between the epochs, being concave (with respect to the centre of the remnant) in the 1985 image, but slightly convex in the 2008 image (labelled ‘R’). If extrapolated, this apparently points towards the faint eastern extension, which corresponds to the

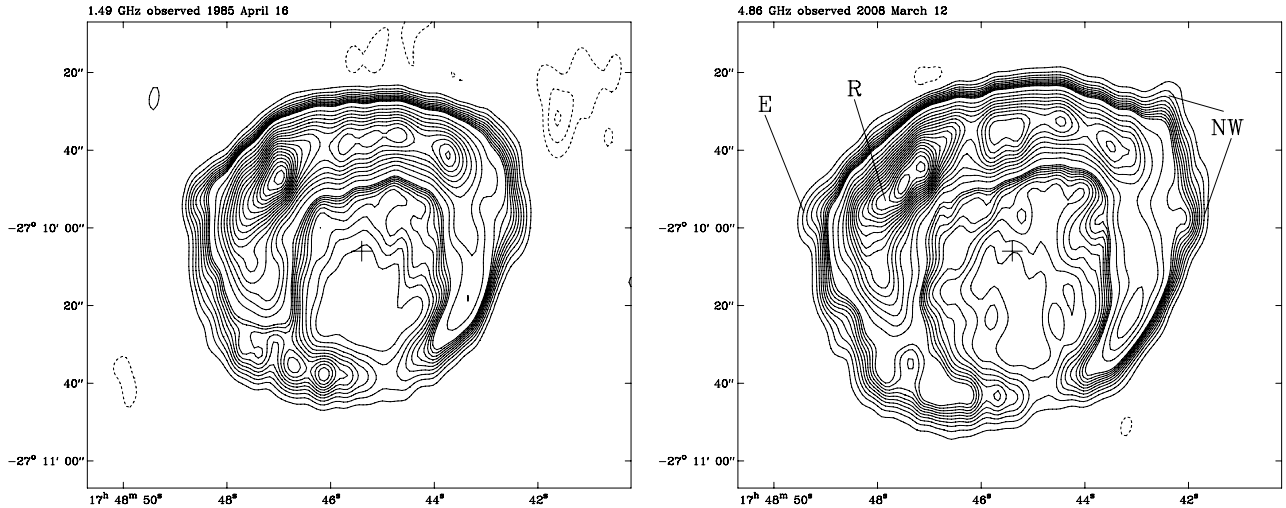


**Figure 1.** VLA observations of G1.9+0.3: (left-hand panel) at 1.49 GHz from 1985 with contour levels at  $(-3, -2, -1, 1, 2, 3 \dots 10, 15, 20 \dots 95) \times 0.30 \text{ mJy beam}^{-1}$ , and (right-hand panel) at 4.86 GHz from 2008 with contour levels at  $(-3, -2, -1, 1, 2, 3 \dots 10, 15, 20 \dots 95) \times 0.17 \text{ mJy beam}^{-1}$ . The negative contours are dashed. Both images have a resolution of  $10 \times 4 \text{ arcsec}^2$  at  $5^\circ 5' \text{ W}$  from N. The central crosses mark the centre position used for radial profiles (see the text and Fig. 2).

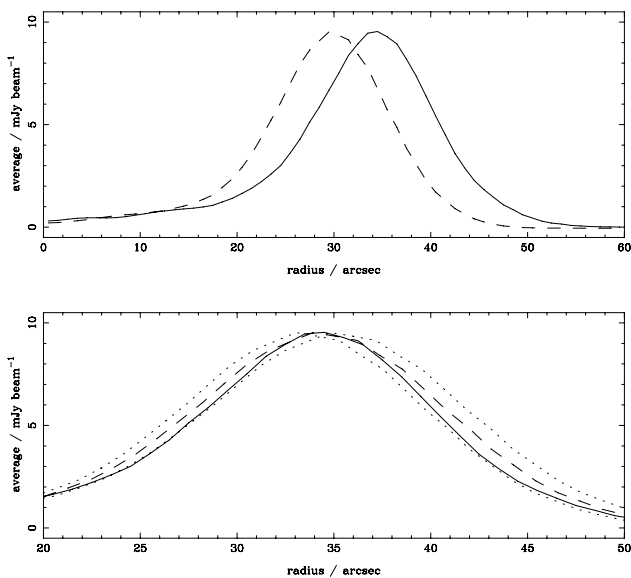


**Figure 2.** Top panel: radial profiles of radio emission from G1.9+0.3, from 1985 (dashed lines) and 2008 (solid lines). Bottom panel: scaled profile from 1985, expanded by 12, 15 and 18 per cent (dotted, dashed and dotted lines), compared with the 2008 profile. (The amplitudes of the profiles from 2008 have been multiplied by 1.65).

northern edge of the X-ray emission outside the main rim in the east. Also, the peaks of the bright ridge of the radio emission change between the two epochs (e.g. the peak in the north-east in the 1985 image splits into two peaks in the 2008 image).

From Figs 1 and 3, there are striking differences between the overall structure of G1.9+0.3 at radio and X-ray wavelengths, which may reflect differences in particle acceleration rates or efficiencies at different locations. Although the outline of the remnant is very nearly circular in the radio, the brightness of the radio emission varies considerably in azimuth (with the bright north-eastern rim being about 50 times brighter than the weakest emission in the south). If a local density gradient were invoked to explain the large north-south difference in radio brightness, then it would not be obvious

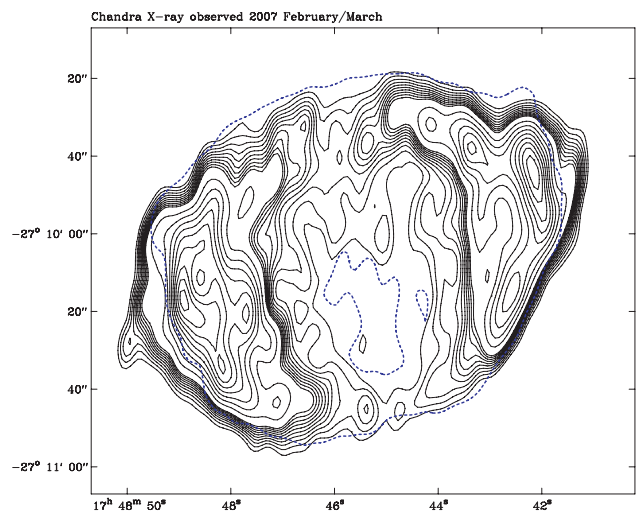


**Figure 3.** The black contours, at  $(2.4, 3.0, 3.6 \dots 7.8, 10.8, 13.8 \dots 34.8) \times 10^{-4} \text{ counts s}^{-1} \text{ beam}^{-1}$ , are *Chandra* X-ray observations of G1.9+0.3 (Paper I), with the same resolution and scale as the radio images shown in Fig. 1. (The background level away from the remnant is  $\approx 1.8 \times 10^{-4} \text{ counts s}^{-1} \text{ beam}^{-1}$ .) The dotted blue contour is the lowest contour of the 2008 4.86-GHz radio image shown in Fig. 1.

why the remnant maintains such a circular outline. On the other hand, the X-ray emission of the remnant shows a bipolar structure, brightest in the east and west, which suggests that the influence of a large-scale magnetic field is important for the efficiency of accelerating the particles responsible for the X-ray emission, but *not* for those producing the radio emission. The brightest emission in the east and particularly in the north-west corresponds to relatively faint radio emission. In the north-west, this is the outer extension seen in the 2008 radio image, which presumably corresponds to the region of the outer shock with the highest velocity.

### 3.2 Brightening

Given that G1.9+0.3 is such an apparently young SNR, then an obvious question is how is its radio flux density evolving with time?

**Table 2.** Radio flux densities for G1.9 + 0.3.

$\nu$ (MHz)	$S$ (Jy)	$\Delta S$ (Jy)	Observation date(s)	Reference	Note
332	2.84	0.10	1986–1989	LaRosa et al. (2000)	
408	1.18	0.07	1969–1971	Clark & Crawford (1974)	<i>a</i>
843	1.0	0.05	1985–1991	Gray (1994a)	<i>b</i>
843	0.986	0.031	1997–2007?	Murphy et al. (2007)	
1400	0.748	0.038	1993–1996	Condon et al. (1998)	c,d
1425	0.935	0.047	2008	This work	<i>c</i>
2695	0.440	0.044	1981–1984?	Reich et al. (1984)	
4850	0.236	0.016	1990	Griffith et al. (1994)	<i>e</i>
4860	0.437	0.022	2008	This work	<i>c</i>
4875	0.2	0.05	1974–1975	Altenhoff et al. (1979)	<i>f</i>
5000	0.20	0.03	≤1975?	Caswell et al. (1975)	<i>g</i>

Notes. <sup>a</sup>The listed flux density error is based on the quoted 5.4 per cent statistical flux scale (for 1-Jy sources), plus 2 per cent due to possible systematic declination variations, added in quadrature.

<sup>b</sup>No flux density error is given, so a nominal value of 5 per cent is used; the observation dates are from Gray (1994b).

<sup>c</sup>These flux densities were obtained from integrations of images, from within a polygon drawn around the remnant after removing a twisted plane fitted to pixels lying around the edge of the polygon (see Green 2007). The integrated flux density was found to vary by less than 1 per cent when a variety of polygons were used, but to be cautious we assume a statistical error of 5 per cent.

<sup>d</sup>The NVSS survey. G1.9 + 0.3 is also listed in the NVSS source catalogue (Version 2.17):  $58.8 \times 33.3$  arcsec<sup>2</sup> in extent, with  $0.7453 \pm 0.0248$  Jy.

<sup>e</sup>The flux density is from the Vizier version (see Ochsenbein et al. 2000) of the PMN Tropical zone catalogue allowing for a general Gaussian width fit (see Griffith & Wright 1993). The published flux density from a fixed width fit is  $0.175 \pm 0.014$  Jy.

<sup>f</sup>The flux densities of the sources in this survey are quoted to the nearest 0.1 Jy, so a flux density error of 0.05 Jy is used.

<sup>g</sup>The flux density error is from adding quoted errors of 10 per cent for uncorrected gain variations, 10 per cent for positional errors (which would lead to underestimates of the true value) and noise of 0.01 Jy, added in quadrature.

Table 2 lists the available flux densities for G1.9 + 0.3 from the literature, and from the new observations presented here. (There is also a flux density for G1.9 + 0.3 at 365 MHz from the Texas survey, Douglas et al. 1996, but this has not been listed as it is not expected that it will represent the total flux of G1.9 + 0.3, which is resolved by the instrument.) The available observations have been made with a variety of instruments and resolutions, and may not be on consistent flux density scales, making direct comparisons difficult. Nevertheless, there is evidence that the flux density of G1.9 + 0.3 has been *increasing* over recent decades.

(i) Gray (1994a) noted that his 843-MHz flux density was larger than expected from extrapolation between the earlier flux densities at 408 MHz and 5.0 GHz. Gray suggested that this discrepancy was due to the fact that the earlier 408-MHz and 5.0-GHz flux densities were derived assuming the source was unresolved by the  $\approx 3$  arcmin beams of both sets of observations, and so the observed peak flux density would underestimate the integrated flux density. However, even if the source were 1.2 arcmin in extent, as it was when identified by Green & Gull (1984), this effect would be less than about 10 per cent for an  $\approx 3$  arcmin beam, which is not sufficient to explain this discrepancy. Also Gray noted that recent – that is, presumably around 1994 – 4.85-GHz observations (from ‘Haynes et al., in preparation’, which we have not been able to identify in the literature) give a flux density of 0.3 Jy for G1.9 + 0.3, which is above the earlier 5.0-GHz flux density reported by Caswell, Haynes & Clark (1975).

(ii) The 332-MHz flux density is considerably larger than the earlier value at 408 MHz (Clark & Crawford). (Note that LaRosa et al. quote a 1.4-GHz flux density from NVSS with an implausibly large error, that is,  $0.747 \pm 0.250$  Jy, and hence also give very large error in their derived 332 MHz to 1.4 GHz spectral index, that is,  $0.93 \pm 0.23$ .)

(iii) The integrated flux density of G1.9 + 0.3 at 4.86 GHz from the observations described above is significantly larger than any of the values available in the literature at similar frequencies, even

bearing in mind the large errors in some of the earlier flux densities at  $\approx 5$  GHz, and the possibility of systematic differences in the flux density scales between the different observations.

(iv) The 1.43-GHz flux density from our recent observations is larger than the previously available value at 1.4 GHz found 13 yr earlier by about a factor of  $1.25 \pm 0.09$ , which implies a flux density increase of  $\sim 2$  per cent yr<sup>-1</sup>.

Combining the integrated flux densities from the contemporaneous, new 1.45- and 4.86-GHz observations gives a spectral index,  $\alpha$ , for the radio emission from G1.9 + 0.3 (here defined in the sense that flux density scales with frequency as  $S \propto \nu^{-\alpha}$ ) of 0.62. The error in this spectral index is  $\pm 0.06$  using the nominal 5 per cent uncertainties in the individual flux densities, not including any possible systematic uncertainties in the relative flux density scales of the observations. However, it is difficult to reconcile this spectral index with all the other observations in the literature. If G1.9 + 0.3 is indeed brightening, then the spectral index between 332 MHz and 1.4 GHz would be larger than the value of 0.93 obtained by LaRosa et al., as the 1.4-GHz observation was obtained after the 332-MHz data. Also, the two 843-MHz flux densities do not show obvious evidence for brightening. Excluding the 332-MHz flux density, it is possible to obtain a reasonable fit of a spectrum with  $\alpha \approx 0.7$  brightening at  $\approx 2$  per cent yr<sup>-1</sup> to the available flux densities for G1.9 + 0.3. The model fits reported in Paper I assumed a flux density at 1 GHz of 0.9 Jy. Increasing this to 1.2 Jy results in slightly steeper values of the radio-to-X-ray spectral index. However, the new values of both the spectral index and the roll-off frequency are still consistent with the earlier values at the 90 per cent confidence level.

The fact that G1.9 + 0.3 is brightening is not unexpected if it is indeed only a 100 yr or so old. Radio observations of SNe show brightening emission over time-scales of up to a year or so after the optical SN due to decreasing opacity. Thereafter, these radio SNe (RSNe) show steady decline in emission (see e.g. Weiler et al. 1986, 2002). Searches for radio emission from older RSNe, up to about

80 yr old (see Eck, Cowan & Branch 2002), mostly provide upper limits for the radio emission, indicating that the luminosities of these older RSNe are less than that of the brightest known Galactic SNR. Thus, in order to evolve to match the observed properties of Galactic SNRs, it is expected that radio emission from young SNRs will brighten, probably on time-scales of about a century, when they have swept up sufficient interstellar medium (e.g. Gull 1973; Cowsik & Sarkar 1984). (SN1987A is brightening at radio wavelengths, as it interacts with a ring of material very near the explosion; Manchester et al. 2002.) For a current angular size of 92 arcsec, and a 1-GHz flux density of 1.2 Jy, the surface brightness of G1.9 + 0.3 is  $\approx 7.7 \times 10^{-20} \text{ W m}^{-2} \text{ Hz}^{-1} \text{ sr}^{-1}$ . This means that G1.9 + 0.3 is brighter than the remnant of the SN of AD 1006, somewhat fainter than the remnants of Tycho's and Kepler's SNe of AD 1572 and 1604, but is considerably fainter than Cas A, which is otherwise the youngest (approximately 300 yr old) and brightest known Galactic SNR (e.g. Green 2004).

Predictions can be made for brightness increases based on simple assumptions about particle acceleration and possible magnetic field amplification. For power-law behaviour of source radius with time, and of ejecta and ambient density with radius, power-law time dependencies can be found for the relativistic particle energy density (assuming a constant efficiency, that is,  $u_e \propto \rho v_s^2$ ), magnetic field (assuming either flux freezing upstream or amplification with a different efficiency), and therefore the synchrotron luminosity:  $S_\nu \propto t^l$ . Once substantial deceleration has begun (i.e. once a reverse shock has formed, within a few years of the explosion), almost all models decrease in luminosity with time. For constant ambient density the drop is slowest; for constant ambient magnetic field as well, the luminosity can actually rise, roughly as  $t^{0.9}$  for the Type Ia SN model of Chevalier (1982); all other cases drop with time. While these are simplistic estimates, they do demonstrate that a *growing* radio flux density requires special conditions.

If G1.9 + 0.3 is now  $\sim 100$  yr old, the observed flux increase by a factor of 1.25 over 13 yr gives  $l = 1.6$ , far larger than the largest estimates above. While other explanations cannot be ruled out, the most natural explanation is that the efficiency with which shock energy goes into relativistic electrons and/or magnetic field must be *increasing with time*.

#### 4 CONCLUSIONS

A comparison of VLA observations made in 1985 and 2008 confirms that G1.9 + 0.3 has a large expansion rate of  $\approx 0.65$  per cent  $\text{yr}^{-1}$ . This means that this is a very young SNR, at most only 150 yr old, and hence the youngest known Galactic SNR. There is also evidence that the this remnant has been brightening over the last few decades at radio wavelengths, suggesting that the efficiency of particle acceleration and/or magnetic field amplification has been increasing. Further high-resolution, multi-epoch radio observations are required to study G1.9 + 0.3's dynamics and structure in detail, and monitor the temporal evolution of its flux density.

#### ACKNOWLEDGMENTS

The National Radio Astronomy Observatory is a facility of the National Science Foundation operated under cooperative agreement by Associated Universities, Inc. We are very grateful to the NRAO for the prompt scheduling of the 'Exploratory Time' proposal for the new VLA observations presented here. This research has made use of NASA's Astrophysics Data System Bibliographic Services.

RP is an employee of the US Federal Government and his contribution to this article is in the public domain (no claim to original US government works).

#### REFERENCES

- Altenhoff W. J., Downes D., Pauls T., Schraml J., 1979, *A&AS*, 35, 23  
 Anderson M. C., Rudnick L., 1995, *ApJ*, 441, 307  
 Bridle A. H., Greisen E. W., 1994, AIPS Memo 87. Available from <http://www.aips.nrao.edu/>  
 Caswell J. L., Haynes R. F., Clark D. H., 1975, *Aust. J. Phys.*, 28, 633  
 Chevalier R. A., 1982, *ApJ*, 258, 790  
 Clark D. H., Crawford D. F., 1974, *Aust. J. Phys.*, 27, 713  
 Condon J. J., Cotton W. D., Greisen E. W., Yin Q. F., Perley R. A., Taylor G. B., Broderick J. J., 1998, *AJ*, 115, 1693  
 Cowsik R., Sarkar S., 1984, *MNRAS*, 207, 745  
 Douglas J. N., Bash F. N., Bozayan F. A., Torrence G. W., Wolfe C., 1996, *AJ*, 111, 1945  
 Eck C. R., Cowan J. J., Branch D., 2002, *ApJ*, 573, 306  
 Gray A. D., 1994a, *MNRAS*, 270, 835  
 Gray A. D., 1994b, PhD thesis, University of Sydney  
 Green D. A., 1985, *MNRAS*, 216, 691  
 Green D. A., 1989, *AJ*, 98, 1358  
 Green D. A., 2004, *BASI*, 32, 335  
 Green D. A., 2005, *MmSAI*, 76, 534  
 Green D. A., 2007, *BASI*, 35, 77  
 Green D. A., Gull S. F., 1984, *Nat*, 312, 527  
 Griffith M. R., Wright A. E., 1993, *AJ*, 105, 1666  
 Griffith M. R., Wright A. E., Burke B. F., Ekers R. D., 1994, *ApJS*, 90, 179  
 Gull S. F., 1973, *MNRAS*, 161, 47  
 Helfand D. J., Chance D., Becker R. H., White R. L., 1984, *AJ*, 89, 819  
 LaRosa T. N., Kassim N. E., Lazio T. J. W., Hyman S. D., 2000, *AJ*, 119, 207  
 Manchester R. N., Gaensler B. M., Wheaton V. C., Staveley-Smith L., Tzioumis A. K., Bizunok N. S., Kesteven M. J., Reynolds J. E., 2002, *PASA*, 19, 207  
 Misanovic Z., Cram L., Green A., 2002, *MNRAS*, 335, 114  
 Morris P. W., Stolovy S., Wachter S., Noriega-Crespo A., Pannuti T. G., Hoard D. W., 2006, *ApJ*, 640, L179  
 Murphy T., Mauch T., Green A., Hunstead R. W., Piestrzynska B., Kels A. P., Sztajer P., 2007, *MNRAS*, 382, 382  
 Nord M. E., Lazio T. J. W., Kassim N. E., Hyman S. D., LaRosa T. N., Brogan C. L., Duric N., 2004, *AJ*, 128, 1646  
 Ochsnein F., Bauer P., Marcout J., 2000, *A&AS*, 143, 23  
 Reich W., Fürst E., Haslam C. G. T., Steffen P., Reif K., 1984, *A&AS*, 58, 197  
 Renaud M., Paron S., Terrier R., Lebrun F., Dubner G., Giacani E., Bykov A. M., 2006, *ApJ*, 638, 220  
 Reynolds S. P., Borkowski K. J., Green D. A., Hwang U., Harrus I., Petre R., 2008, *ApJL*, in press (arXiv:0803.1487) (Paper I)  
 Reynoso E. M., Moffett D. A., Goss W. M., Dubner G. M., Dickel J. R., Reynolds S. P., Giacani E. B., 1997, *ApJ*, 491, 816  
 Saikia D. J., Thomasson P., Roy S., Pedlar A., Muxlow T. W. B., 2004, *MNRAS*, 354, 827  
 Sakano M., Koyama K., Murakami H., Maeda Y., Yamauchi S., 2002, *ApJS*, 138, 19  
 Sramek R. A., Cowan J. J., Roberts D. A., Goss W. M., Ekers R. D., 1992, *AJ*, 104, 704  
 Tan S. M., Gull S. F., 1985, *MNRAS*, 216, 949  
 The L.-S. et al., 2006, *A&A*, 450, 1037  
 Weiler K. W., Sramek R. A., Panagia N., van der Hulst J. M., Salvati M., 1986, *ApJ*, 301, 790  
 Weiler K. W., Panagia N., Montes M. J., Sramek R. A., 2002, *ARA&A*, 40, 387  
 Yusef-Zadeh F., Hewitt J. W., Cotton W., 2004, *ApJS*, 155, 421

This paper has been typeset from a  $\text{\TeX}/\text{\LaTeX}$  file prepared by the author.